

# Examining the potential of Sentinel-2 MSI spectral resolution in quantifying above ground biomass across different fertilizer treatments



Mbulisi Sibanda\*, Onesimo Mutanga, Mathieu Rouget

School of Agricultural, Earth and Environmental Sciences, University of KwaZulu-Natal, P/Bag X01, Scottsville, 3209 Pietermaritzburg, South Africa

## ARTICLE INFO

### Article history:

Received 17 June 2015

Received in revised form 9 October 2015

Accepted 26 October 2015

Available online 14 November 2015

### Keywords:

Field spectroscopy

New generation multispectral sensors

Rangeland fertilization

Spectral resampling

## ABSTRACT

The major constraint in understanding grass above ground biomass variations using remotely sensed data are the expenses associated with the data, as well as the limited number of techniques that can be applied to different management practices with minimal errors. New generation multispectral sensors such as Sentinel 2 Multispectral Imager (MSI) are promising for effective rangeland management due to their unique spectral bands and higher signal to noise ratio. This study resampled hyperspectral data to spectral resolutions of the newly launched Sentinel 2 MSI and the recently launched Landsat 8 OLI for comparison purposes. Using Sparse partial least squares regression, the resampled data was applied in estimating above ground biomass of grasses treated with different fertilizer combinations of ammonium sulfate, ammonium nitrate, phosphorus and lime as well as unfertilized experimental plots. Sentinel 2 MSI derived models satisfactorily performed ( $R^2 = 0.81$ , RMSEP = 1.07 kg/m<sup>2</sup>, RMSEP<sup>-rel</sup> = 14.97) in estimating grass above ground biomass across different fertilizer treatments relative to Landsat 8 OLI (Landsat 8 OLI:  $R^2 = 0.76$ , RMSEP = 1.15 kg/m<sup>2</sup>, RMSEP<sup>-rel</sup> = 16.04). In comparison, hyperspectral data derived models exhibited better grass above ground biomass estimation across complex fertilizer combinations ( $R^2 = 0.92$ , RMSEP = 0.69 kg/m<sup>2</sup>, RMSEP<sup>-rel</sup> = 9.61). Although Sentinel 2 MSI bands and indices better predicted above ground biomass compared with Landsat 8 OLI bands and indices, there were no significant differences ( $\alpha = 0.05$ ) in the errors of prediction between the two new generational sensors across all fertilizer treatments. The findings of this study portrays Sentinel 2 MSI and Landsat 8 OLI as promising remotely sensed datasets for regional scale biomass estimation, particularly in resource scarce areas.

© 2015 International Society for Photogrammetry and Remote Sensing, Inc. (ISPRS). Published by Elsevier B.V. All rights reserved.

## 1. Introduction

Optimizing the productivity of natural rangelands through fertilization has become a global norm especially in sub-Saharan Africa where livestock farming is limited by the lack of quality forage resources (Vickery et al., 1980; Valentin et al., 2014). Fertilizer application is critical in restoring the quality and quantity of native rangelands or pastures for high livestock production (Vogeler et al., 2014; Quan et al., 2015). Moreover, the higher the grass quantity, the greater the potential of supplementary carbon sinks and soil protection mechanism among other factors (Prado et al., 2014). There is ample literature that indicates an increment in the productivity of natural grasslands or pastures after the application of fertilizers (Ghani et al., 2014; Trotter et al., 2014; Vogeler et al., 2014). However, there are remarkable discrepancies in the extent

of productivity reported by these studies. This is largely due to great variations in the methods used, fertilizer type, soil fertility, amount of rainfall, temperature variations, differences in grass species, management practices (Wight and Godfrey, 1985; Jørgensen et al., 2014) and most importantly the lack of reliable primary spatial data sources (Jørgensen et al., 2014; Porter et al., 2014).

Remote sensing is an alternative primary data source that can contribute to a better understanding of the effect of fertilizer application on grass productivity since it offers instantaneous and spatially explicit patterns of ecosystem changes and variations (Abbasi et al., 2014). Specifically, attention has been focused on the use of nitrogen for pasture or grassland fertilization (Richardson et al., 1983; Wight and Godfrey, 1985; Kooistra et al., 2010; Ramoelo et al., 2013; Ling et al., 2014; Yahdjian et al., 2014; Mutanga et al., 2015). For instance, Ling et al. (2014) used hyperspectral datasets to estimate canopy nitrogen of prairie tall grass and concluded that empirical methods based on hyperspectral data can be used to optimally estimate grass canopy nitrogen. Similar studies

\* Corresponding author.

E-mail address: [sibandambulisi@gmail.com](mailto:sibandambulisi@gmail.com) (M. Sibanda).

were also done to estimate grass biomass using hyperspectral data (Mutanga and Skidmore, 2004a; Mutanga and Adam, 2011). However, hyperspectral data is very expensive and spatially restricted (Tong et al., 2014). There is therefore, a need to identify cheap data sources that would permit regional estimation.

An increasing body of contemporary literature shows the potential of multispectral remotely sensed data in rangeland studies (Serrano et al., 2002; Ramoelo et al., 2012; Ullah et al., 2012). The major motivation for their usage is their free availability to resource constrained regions (Lu, 2006). Besides, most multispectral remotely sensed datasets are characterized with high temporal resolutions and wide swath widths making them suitable for regional applications (Lu, 2005; Li et al., 2014). In spite of these advantages, some studies discredited the utility of multispectral data in remote sensing plant biomass and biochemical properties (Broge and Mortensen, 2002). The broad bandwidths and low spectral resolutions of multispectral data were often cited to be insensitive to differences in plant characteristics (Elvidge and Chen, 1995; Broge and Leblanc, 2001; Curran, 2001; Hansen and Schjoerring, 2003; Mutanga and Skidmore, 2004b; Underwood et al., 2007).

The upcoming space borne multispectral sensors with improved bandwidths and spectral resolutions are hypothesized to have a great potential in a wide range of vegetation mapping applications (Oumar and Mutanga, 2013). For instance, the forthcoming Sentinel 2 Multi-Spectral Imager (MSI) is perceived to have a great potential of facilitating the development of a variety of applications including assessing the effect of plant fertilizer applications. The advent of Sentinel coincides with the growing interest from the agricultural sector of coming up with accurate and affordable spatial datasets and techniques for assessing different agricultural management practices at regional scales (Moran et al., 1997; Haboudane et al., 2002). The forthcoming Sentinel 2 MSI is a polar orbiting sensor comprised of two satellites, each carrying a MSI characterized by 290-km swath width, potentially suitable for regional mapping in rangeland management. This sensor offers a multipurpose design of 13 spectral bands traversing from the visible and near infrared up to the shortwave infrared. In total, Sentinel 2 MSI has four bands (2, 3, 4 and 8) with a spatial resolution of 10 m, six bands (5, 6, 7, 8a, 11 and 12) at 20 m and the final three bands (1, 9 and 10) at 60 m. Among the thirteen Sentinel 2 MSI bands, there are three novel bands in the red-edge region positioned at 705, 740 and 783 nm, a component that previous multispectral sensors lacked. These bands are presumed to have a high potential for mapping various vegetation characteristics. For instance, Ramoelo et al. (2014) successfully demonstrated the potential of Sentinel 2 MSI's red edge bands in estimating grass nutrients. The sensor is expected to provide data acquired over land and coastal zones. Consequently, the three new Sentinel 2 MSI bands in the red edge region could be useful in estimating grass productivity particularly in data scarce regions of the sub-Saharan Africa.

To ascertain the full potential of Sentinel 2 MSI sensor in estimating grass above ground biomass, there is need to compare its performance to other satellite datasets particularly the Landsat 8 and hyperspectral. A comparison of grass above ground biomass estimation accuracies of Sentinel 2 MSI with those of the newly launched Landsat 8 operational land imager can illustrate the utility and the predictive strength of this sensor in sustainable rangeland management particularly in resources scarce areas as Southern Africa. Landsat 8 OLI is one of the two instruments on board Landsat 8 satellite offering nine bands with a great potential of estimating grass above ground biomass. Although this sensor has not been fully utilized in grassland studies, so far its application in forests has demonstrated that it is more robust in predicting above ground biomass (Dube and Mutanga, 2015a, b). Considering

that no study has sought to evaluate the utility of Sentinel 2 MSI in estimating rangeland grass above ground biomass across different fertilizer applications, a comparative study of this sensor and other readily available sensors such as Landsat 8 OLI is critical in evaluating its utility for regional scale rangeland management applications.

The use of these remotely sensed datasets in conjunction with efficient and robust prediction algorithms could provide critical tools for assessing rangeland condition across different management practices at regional scales. One of the renowned prediction algorithms that contemporary remote sensing scientists (Abdel-Rahman et al., 2014) advocate for is the Sparse Partial Least Squares Regression (SPLSR) algorithm (Chun and Keleş, 2010). This algorithm has a capacity to screen greatly correlated data without over-fitting its prediction models (Lee et al., 2011). In addition, SPLSR has the capacity to select best predictor variables as compared to its predecessor, partial least squares regression analysis (PLSR) (Abdel-Rahman et al., 2014). The aforementioned robustness of SPLS makes it an ideal algorithm for assessing the productivity of native grasslands treated with complex fertilizer treatments. The aim of this study was to explore the utility of the forthcoming new generation multispectral sensor Sentinel 2 MSI bands and indices in estimating grass above ground biomass across complex fertilizer treatments. To explore the utility of Sentinel 2 MSI in estimating grass above ground biomass, this study compared the results of Sentinel-2 MSI resampled data with those of hyperspectral and the simulated Landsat 8 OLI spectral bands. The simulated Landsat 8 OLI spectral bands were also used because of the sensor's spatial fidelity and the improved signal to noise ratio (Dube and Mutanga, 2015a).

## 2. Materials and methods

### 2.1. Study area

The study was conducted using experimental plots established by J.D. Scott in 1950 (Morris and Fynn, 2001) at Ukulinga (University of KwaZulu-Natal Research Farm) in Pietermaritzburg, South Africa, (29°24'E, 30°24'S) (see Fig. 1). In this study, only the grass growing season of October 2013 to April 2014 was considered. The grass species prevalent in the experimental plots include *Themeda triandra*, *Heteropogon contortus*, *Eragrostis plana*, *Panicum maximum*, *Setaria nigrirostris* and *Tristachya leucothrix*. The height of the grasses ranged between 25 and 30 cm. Generally, temperatures range from 23 to 33 °C during summer and 16 to 25 °C during winter in Pietermaritzburg. The soils at Ukulinga are grouped under the, acidic Westleigh form (plinthic 2 paleustalf) group which is relatively infertile (Fynn and O'Connor, 2005).

### 2.2. Experimental design

In this study, 96 experimental plots with a length of 9 m and a width of 3 m were used. In all these plots, 11 fertilizer combinations and the "control" (untreated grass) were used to treat the grass in this experiment as shown in Table 1. An amount of zero and 33.6 g m<sup>-2</sup> of dolomite lime treatments were applied every fifth year, super phosphate applied every year at zero and 225 g m<sup>-2</sup> as well as two ammonium fertilizers (ammonium nitrate and ammonium sulfate), each applied every year at four levels. In this experiment, ammonium nitrate was combined with lime and phosphorus but not with ammonium sulfate considering the fact that they are both nitrogenous fertilizers. All treatments were randomly assigned to each plot within the three replicates or blocks.

**Table 1**  
Field measured reflectance samples.

| Treatment group | Fertilizer combinations | Abbreviation | No. of plots | No. of samples |
|-----------------|-------------------------|--------------|--------------|----------------|
| 1               | “Control” (C)           | C            | 6            | 48             |
| 2               | Ammonium Nitrate (AN)   | AN           | 9            | 72             |
| 3               | AN + Lime               | ANL          | 9            | 72             |
| 4               | AN + Phosphorous (P)    | ANP          | 9            | 72             |
| 5               | AN + Lime (L) + P       | ANLP         | 9            | 72             |
| 6               | Ammonium Sulfate (AS)   | AS           | 9            | 72             |
| 7               | AS + L                  | ASL          | 9            | 72             |
| 8               | AS + P                  | ASP          | 9            | 72             |
| 9               | AS + L + P              | ASLP         | 9            | 72             |
| 10              | P                       | P            | 6            | 48             |
| 11              | L                       | P            | 6            | 48             |
| 12              | L + P                   | LP           | 6            | 48             |
| Total           |                         |              | 96           | 768            |

AN = ammonium nitrate; AS = ammonium sulfate; L = lime; and PL = phosphorus combined with lime.

### 2.3. Grass above ground biomass data

To derive grass above ground biomass, the fertilized grasses in the 96 plots were harvested at the end of the grass growing season in April 2014. After harvesting, representative samples were selected from each plot, oven dried and reweighed to derive the dry biomass. These measurements were then transformed to derive total above ground biomass for each plot in kilograms per plot (kg/plot).

### 2.4. Remotely sensed data

For this study, hyperspectral data as well as Sentinel 2 MSI and Landsat 8 OLI data resampled from hyperspectral data were used to estimate grass above ground biomass. Field grass spectral reflectance was measured using an Analytical Spectral Device (ASD) FieldSpec instrument within the 96 plots, treated with different fertilizer treatments. In each of the 96 plots, eight spectra were measured resulting in a total of 768 samples (Table 1). The ASD spectrometer records radiation at 1.4 nm intervals for the spectral region 350–1000 nm and 2 nm intervals for the spectral region 1000–2500 nm. Spectral measurements were conducted under clear sky conditions between 10 am and 2 pm because this is the period of day with the maximum radiation from the sun. In measuring grass reflectance, bare fiber-optic sensor connected to the hyperspectral spectro-radiometer was held at a nadir position approximately 1 m above grass canopies (Abdel-Rahman et al., 2014; Mutanga et al., 2015). Consequently a ground view of

approximately 0.45 m in diameter, ample to capture the reflectance of grass canopy was covered (Abdel-Rahman et al., 2014). When measuring the spectra, fiber optic cable was held at an arm's length away from the person recording so as to avoid the influence of the recorder's shadow and clothing on the registered grass canopy spectra. Moreover the spectra were collected after the green peak stage when the grasses were mature. Spectrometer measurements were standardized after every 5–10 spectra measurements using a standard spectral on to regulate possible atmospheric condition changes and sun irradiance (Abdel-Rahman et al., 2014).

To simulate Sentinel-2 MSI, 768 grass reflectance samples measured in the 96 plots treated with different fertilizer combinations were then resampled based on the bandwidths of the thirteen bands illustrated in Table 2 as in Delegido et al. (2011) and Ramoelo et al. (2014). The two instruments from the European Space Agency (ESA), Sentinel 2A launched on the 23 of June and Sentinel 2B yet to be launched in 2016, are dedicated to monitor land and coastal areas (Lachérade et al., 2014; Laurent et al., 2014; van der Meer et al., 2014). According to ESA, the two sensors will have a revisit time of 5 days, placed at an orbital angular distance of 180° with a field of view of 290 km (Cole et al., 2014). It is expected that it would acquire all its images at a nadir position at thirteen spectral wavelengths ranging from visible through the most promising red edge bands to the short wave infrared wavelengths as listed in Table 2 with a high spatial resolution ranging from 10 to 60 m.

To simulate the spectral resolution of Landsat 8 OLI, hyperspectral data, measured in the 96 plots treated with different fertilizer combinations was averaged based on the bandwidths of the seven bands illustrated on Table 2. Launched in 2013, the operational land imager (OLI) and the thermal infrared sensor (TIRS) are the two instruments on board Landsat 8 satellite. These two instruments capture images of the earth at 16 day temporal resolution with a scene size of about 170 km by 183 km, suitable for regional vegetation mapping applications. Although the spectral bands of OLI sensor are similar to those of Landsat 7 ETM+, OLI sensors has two new bands and an advanced signal to noise radiometric performance which gives it a great potential for agricultural applications.

#### 2.4.1. Variables for predicting grass above ground biomass

To test the utility of Sentinel 2 MSI in estimating grass above ground biomass relative to Landsat OLI and hyperspectral sensors, raw bands and several vegetation indices were used. Table 3 shows the specific calculated broad and narrow band vegetation indices. The vegetation indices used in this study were selected based on their performance in previous grass biomass and grass nutrients

**Table 2**  
Spectral and spatial resolutions of Sentinel 2 MSI and Landsat 8 OLI.

| Sentinel 2 MSI |                  |                |                        | Land sat 8 OLI  |                        |
|----------------|------------------|----------------|------------------------|-----------------|------------------------|
| Spectral bands | Band center (nm) | Bandwidth (nm) | Spatial resolution (m) | Band range (nm) | Spatial resolution (m) |
| B1             | 443              | 20             | 60                     | 0.435–0.451     | 30                     |
| B2             | 490              | 65             | 10                     | 0.452–0.512     | 30                     |
| B3             | 560              | 35             | 10                     | 0.533–0.590     | 30                     |
| B4             | 665              | 30             | 10                     | 0.636–0.673     | 30                     |
| B5             | 705              | 15             | 20                     | 0.851–.879      | 30                     |
| B6             | 740              | 15             | 20                     | 1.566–1.651     | 30                     |
| B7             | 783              | 20             | 20                     | 2.107–2.294     | 30                     |
| B8             | 842              | 115            | 10                     | 0.503–0.676     | 15                     |
| B8a            | 865              | 20             | 20                     |                 |                        |
| B9             | 945              | 20             | 60                     | 1.363–1.384     | 30                     |
| B10            | 1375             | 30             | 60                     | 10.60–11.19     | 100                    |
| B11            | 1375             | 30             | 20                     | 11.50–12.51     | 100                    |
| B12            | 2190             | 180            | 20                     |                 |                        |

**Table 3**

Variables used in predicting above ground biomass of grasses treated with different fertilizer.

| Analysis stage | Variables          | Sensor  | Spectral bands   |
|----------------|--------------------|---|--|
| 1              | Raw bands          | Hyper spectral<br>Sentinel 2 MSI<br>Landsat 8 OLI     | Band 400–1355, 1421–1809, 1941–2469 (1326 bands)<br>Visible (bands 1, 2, 3, 4), red edge(bands 5, 6, 7, 8, 8a), shortwave infrared (bands 9 and 12)<br>Visible (bands 1 2 3 4) near infrared (bands 5) shortwave infrared (6 7 8) (8bands) |
| 2              | Vegetation indices | Hyper spectral<br><br>Sentinel 2 MSI<br>Landsat 8 OLI | NDVI, PSRI SR3 VOG MCARI MTVI MTVI SAVI RDVI MSR REP_Guy, VREI MRESR MTVI RDVI MSR<br>TCARI<br>NDVI<br>NDVI  |
| 3              | Bands and indices  | Combination of optimal bands and Indices              |  |

NDVI: Normalized Difference Vegetation Index, PSRI: Plant Senescent Reflection Index, SR: Simple Ratio, VOG: Volgaman Index, MCARI: Modified Chlorophyll Absorption Ratio Index, MTVI: Modified Triangle Vegetation Index, REP Guy: Red edge position Guyot, SAVI: Soil Adjusted Vegetation Index, VREI: Volgman Red Edge Index, MRESR: Modified Red Edge Simple Ratio, MTVI: Modified Triangle Vegetation Index, RDVI: Renormalized Difference Vegetation Index, TCARI: Transformed chlorophyll Absorption in Reflectance Index. The vegetation indices used in this study were selected based on their performance in previous grass biomass and grass nutrients estimation studies (Anderson et al., 1993; Broge and Leblanc, 2001; Mutanga and Skidmore, 2004b; Liu et al., 2007; Cho et al., 2008; Agapiou et al., 2012; Thenkabail et al., 2013).

estimation studies (Anderson et al., 1993; Broge and Leblanc, 2001; Mutanga and Skidmore, 2004b; Liu et al., 2007; Cho et al., 2008; Agapiou et al., 2012; Thenkabail et al., 2013).

### 2.5. Statistical analysis

Prior to statistical analysis, exploratory data analysis was conducted to understand the data. Descriptive statistics were generated in Statistica 6 by testing for normality based on the Lilliefors test, prior to regression analysis. The null hypothesis we tested was that the data does not significantly ( $\alpha = 0.05$ ) deviate from the normal distribution.

#### 2.5.1. Sparse partial least squares regression (SPLS)

Sparse partial least squares regression (SPLSR) proposed by Chun and Keleş (2010) was used in this study. Similar to partial least squares regression, SPLSR transforms the variables to new orthogonal factors (components) in order to overcome multicollinearity and over-fitting challenges. When SPLSR is transforming the data, it enforces sparsity and picks out suitable variables for estimating the item of interest. This capability makes SPLSR a unique technique for evaluating highly correlated hyperspectral data. The hypothesis tested was that, the forthcoming new generation Sentinel-2 sensor can estimate above ground biomass with a higher accuracy than the Landsat 8 OLI and can yield comparable results to those obtained using hyperspectral data. Our interest in this study was to use SPS to derive universal bands and indices that could optimally predict grass above ground biomass across different fertilizer treatments.

#### 2.5.2. Evaluation of grass above ground biomass predictions

To evaluate the SPLSR models, a leave-one-out cross validation (LOOCV) method was used as explained in literature (Abdel-Rahman et al., 2014 and Richter et al., 2012). The cross validation method is efficient in cases where the available data samples are limited. In performing the LOOCV method, the data was divided into  $n$  samples (which are 768 in the present study) which were then eliminated one by one. Prediction errors related to a certain number of SPLSR latent components were computed from the predictions attained from the leave-one-out cross validation. These were then used to ascertain the number of components to be used in estimating grass above ground biomass. To assess and evaluate the accuracy and performance of the models, the LOOCV root mean square error of prediction (RMSEP), relative root mean square error (RMSEP<sup>rel</sup>), coefficient of determination ( $R^2$ ) as well as Bias were computed. The use of raw spectral bands and vegetation indices

that yielded the lowest RMSEP in all the stages of the analysis were then used in stage three (i.e. combination of optimal bands and indices) of the analysis. To test whether there were significant differences ( $\alpha = 0.05$ ) between prediction errors of all the sensors, we calculated and used the confidence intervals of RMSEP. The RMSEP were derived using the selected raw spectral bands and vegetation indices that could optimally estimate grass above ground biomass across all fertilizer treatments. Models which resulted from components that yielded the lowest RMSE of prediction (RMSEP), higher  $R^2$  and low levels of bias were selected and used for predicting grass above ground biomass. To evaluate the contribution of wavelengths to the selected components, loadings or variable importance (VIP) scores derived using SPLSR algorithm were used. Wavelengths that had a loading or VIP score greater than one were deemed to be highly influential and were selected while those with values less than zero were discarded (Abdel-Rahman et al., 2014).

#### 2.5.3. Grass above ground biomass prediction stages

In comparing the spectral resolution robustness of Sentinel 2 MSI to Landsat 8 OLI and hyperspectral data, statistical analysis was conducted at three stages illustrated on Table 3 as follows:

- Raw bands of Sentinel 2 MSI and Landsat 8 OLI, resampled from hyperspectral data as well as the original hyperspectral data were regressed with field measured grass biomass using SPLSR. The component or latent variable that yielded the least possible estimation error (RMSEP) was selected as the best above ground biomass predictor. The SPLSR algorithm selected very important (VIP) variables that optimally estimated grass above ground biomass based on the loading or contribution of each band to the latent variable with the least estimation error.
- Vegetation indices derived from Sentinel 2 MSI and Landsat 8 OLI resampled from hyperspectral data and the original hyperspectral data were also regressed with field measured grass above ground biomass using SPLSR. The vegetation indices that were selected as the best above ground biomass predictors were again selected based on the criteria explained in item one above.
- The bands and indices selected in stages two and three as optimal variables were then combined together and regressed using SPLSR to further select the variables that could optimally estimate above ground biomass across all fertilizer treatments following the criteria explained in item one.



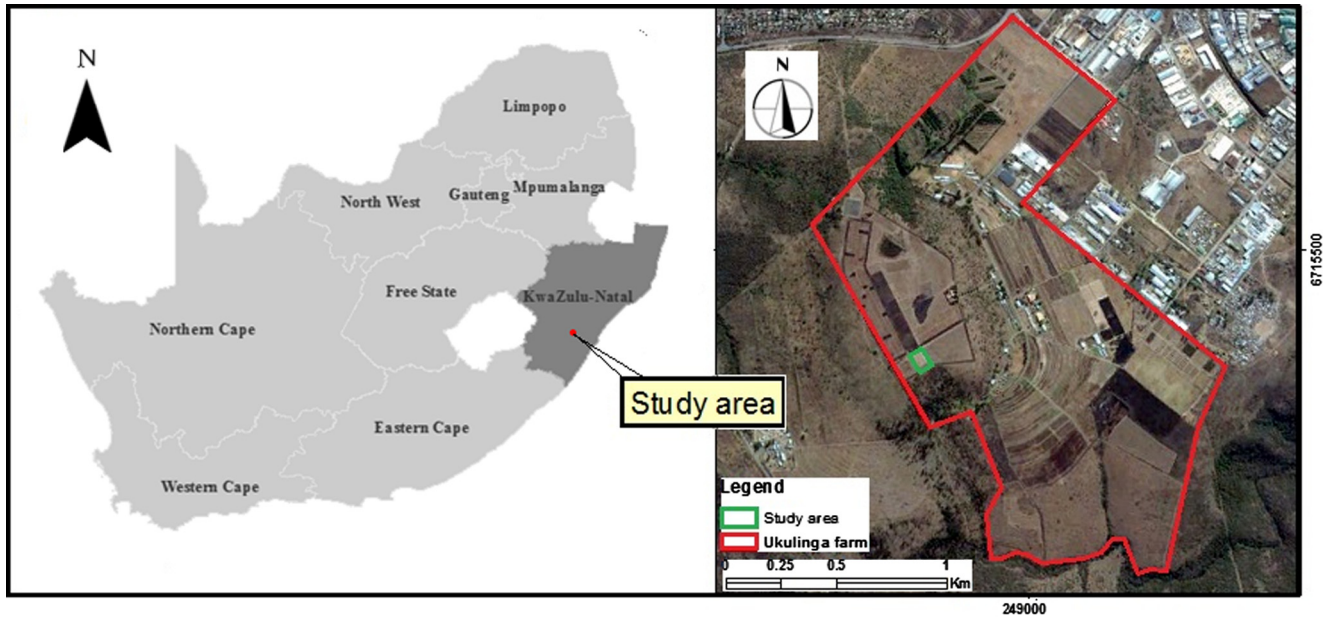


Fig. 1. Ukulinga grassland trails, UKZN farm, Pietermaritzburg, South Africa (Image source: Google Earth).

### 3. Results

#### 3.1. Grass above ground biomass descriptive statistics and analysis of variance test

Exploratory analysis showed that the average grass above ground biomass from the 96 plots was 7.17 Kg, with a minimum of 2.07 Kg and a maximum of 15 Kg. Following the normality test, grass above ground biomass data did not significantly deviate from the normal distribution (Fig. 2). Analysis of variance test results exhibited significant differences in the amount of grass above ground biomass across different fertilizer treatments. Based on post hoc test, there were no significant differences ( $\alpha = 0.05$ ) in the amount of grass above ground biomass among plots treated with Ammonium nitrate, Ammonium sulfate, Phosphorus, Lime Ammonium sulfate combined with lime fertilizers and the “control” (Table 4).

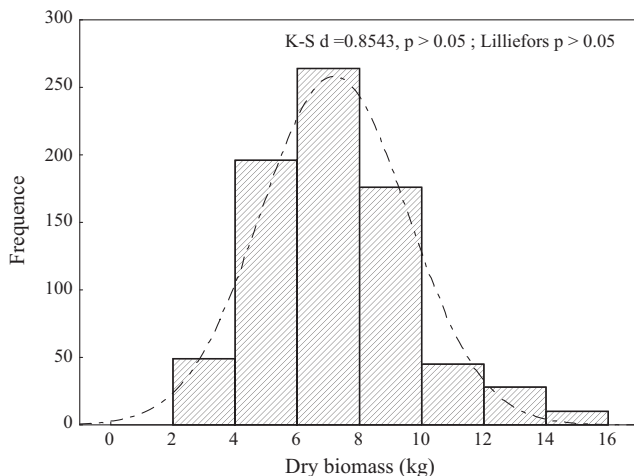


Fig. 2. Dry grass above ground biomass data is not significantly ( $\alpha > 0.05$ ) deviating from the normal distribution based on the Lilliefors and Kolmogorov Smirnov tests of normality.

#### 3.2. Performance of Sentinel 2 MSI in grass above ground biomass estimation relative to Landsat OLI and hyperspectral data

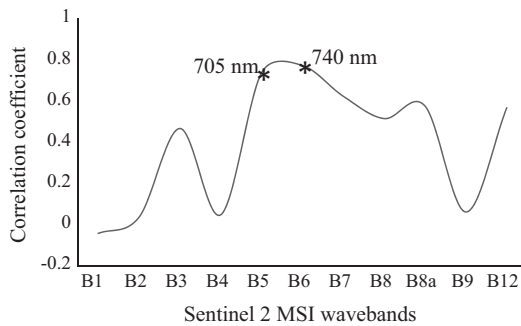
Fig. 3 is a correlogram illustrating the correlation between various Sentinel 2 MSI wavebands and grass biomass. Strong correlations between grass biomass and red edge bands (bands 5, 6, and 7) as well as NIR (8) bands can be observed in the correlogram. It can be observed from the correlogram that bands from the visible region exhibited generally poor correlations to grass biomass. Fig. 4 (a and c) shows that generally, Sentinel 2 MSI optimally estimated above biomass better than Landsat 8 OLI and performed somewhat comparable to hyperspectral bands. For example, using Sentinel 2 MSI raw bands, it can be observed that grasses treated with ammonium sulfate ( $R^2 = 0.67$ , RMSEP = 0.90 kg/m<sup>2</sup>, RMSEP<sub>rel</sub> = 15.41), “control” ( $R^2 = 0.64$ , RMSEP = 0.65 kg/m<sup>2</sup>, RMSEP<sub>rel</sub> = 12.1), ammonium nitrate ( $R^2 = 0.58$ , RMSEP = 0.8809 kg/m<sup>2</sup>, RMSEP<sub>rel</sub> = 15.29) and ammonium sulfate ( $R^2 = 0.69$ , RMSEP = 0.9005 kg/m<sup>2</sup>, RMSEP<sub>rel</sub> = 15.41) fertilizers exhibited the least prediction errors. On the other hand, when using raw Landsat 8 OLI bands, “control” ( $R^2 = 0.43$ , RMSEP = 0.6442 kg/m<sup>2</sup>, RMSEP<sub>rel</sub> = 11.93), ammonium nitrate ( $R^2 = 0.22$ , RMSEP = 1.0422 kg/m<sup>2</sup>, RMSEP<sub>rel</sub> = 23.7), ammonium nitrate combined with lime ( $R^2 = 0.47$ , RMSEP = 1.13 kg/m<sup>2</sup>, RMSEP<sub>rel</sub> = 19.09) and ammonium sulfate combined with lime ( $R^2 = 0.37$ , RMSEP = 1.14 kg/m<sup>2</sup>, RMSEP<sub>rel</sub> = 16.90) had the least prediction errors. Based on hyperspectral data, the grasses treated with ammonium nitrate combined with phosphorous ( $R^2 = 0.60$ , RMSEP = 0.1712 kg/m<sup>2</sup>, RMSEP<sub>rel</sub> = 2.2), ammonium sulfate combined with phosphorous ( $R^2 = 0.69$ , RMSEP = 0.52 kg/m<sup>2</sup>, RMSEP<sub>rel</sub> = 6.1), “control” ( $R^2 = 0.66$ , RMSEP = 0.52 kg/m<sup>2</sup>, RMSEP<sub>rel</sub> = 9.43) and lime ( $R^2 = 0.65$ , RMSEP = 0.6391 kg/m<sup>2</sup>, RMSEP<sub>rel</sub> = 11.6) had the least prediction errors. When the treatments were pooled together, hyperspectral data yielded the lowest errors of prediction. ( $R^2 = 0.73$ , RMSEP = 1.1837 kg/m<sup>2</sup>, RMSEP<sub>rel</sub> = 16.51) relative to Landsat 8 OLI ( $R^2 = 0.56$ , RMSEP = 1.39 kg/m<sup>2</sup>, RMSEP<sub>rel</sub> = 21.36) and Sentinel 2 MSI ( $R^2 = 0.65$ , RMSEP = 1.45 kg/m<sup>2</sup>, RMSEP<sub>rel</sub> = 20.18) (Fig. 4a and c). Although hyperspectral bands optimally estimated above grass biomass, overall, it can be observed that its prediction errors are comparable to those of new generation sensor bands.

**Table 4**

Analysis of variance test results based on Fisher's Least significant difference post hoc test of dry grass above ground biomass.

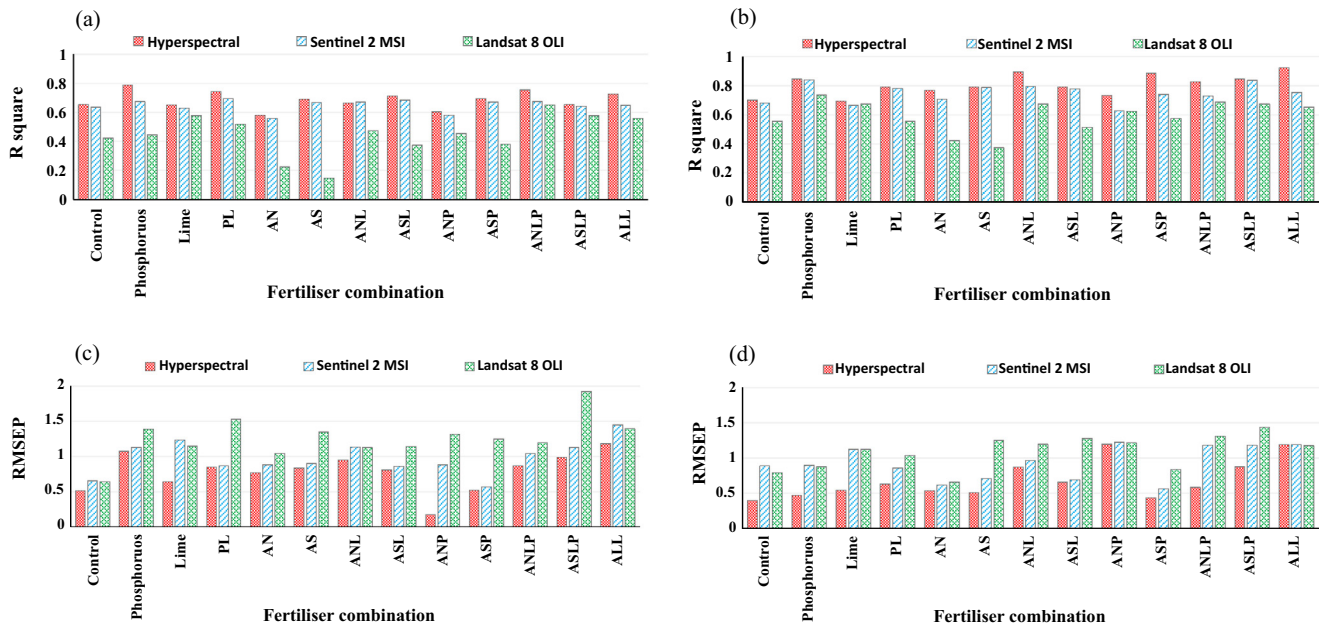
|           | "Control" | AN | AS | P  | Lime | ANL | ASL | PL | ANLP | A_S_L_P | A_P | ASP |
|-----------|-----------|----|----|----|------|-----|-----|----|------|---------|-----|-----|
| "Control" |           | -  | -  | -  | -    | *   | *   | *  | **   | **      | **  | **  |
| AN        | -         |    | -  | -  | -    | -   | **  | *  | **   | **      | **  | **  |
| AS        | -         | -  |    | -  | -    | -   | *   | *  | **   | **      | **  | **  |
| P         | -         | -  | -  |    | -    | -   | *   | *  | **   | **      | **  | **  |
| Lime      | -         | -  | -  | -  |      | -   | *   | *  | **   | **      | **  | **  |
| ANL       | *         | ** | *  | *  | *    |     | -   | -  | **   | **      | **  | **  |
| ASL       | **        | ** | *  | *  | *    | -   |     | -  | **   | **      | **  | **  |
| PL        | **        | ** | *  | *  | *    | -   | -   |    | **   | **      | **  | **  |
| ANLP      | **        | ** | ** | ** | **   | **  | **  | *  |      | *       | -   | -   |
| ASLP      | **        | ** | ** | ** | **   | **  | **  | *  | *    |         | -   | -   |
| ANP       | **        | ** | ** | ** | **   | **  | **  | *  | *    | *       |     | -   |
| ASP       | **        | ** | ** | ** | **   | **  | **  | *  | *    | *       | *   |     |

AN = ammonium nitrate; AS = ammonium sulfate; L = lime; and PL = phosphorus combined with lime.

\* Denote significant differences  $\alpha$  at 0.05.\*\* Denote significant differences  $\alpha$  at 0.01 based on the Fisher's Least Significant Difference post hoc test.**Fig. 3.** Relationship between Sentinel 2 MSI bands and grass biomass using the entire dataset, with bands 5 (centered at 705 nm) and 6 (centered at 740 nm) showing the highest correlation coefficient.

3.3. Performance of the resampled Sentinel 2 MSI derived vegetation indices in grass above ground biomass estimation relative to the performance of Landsat 8 OLI and hyper spectral derived vegetation indices

Fig. 4(b and d) illustrates accuracies attained in estimating grass above ground biomass using vegetation indices derived using Sentinel 2 MSI, Landsat 8 OLI, and hyperspectral data. It can be noted that Sentinel 2 MSI derived vegetation indices optimally estimated above ground biomass of grasses treated with different fertilizer treatments relative to the Landsat 8 OLI. Specifically, the fertilizer treatments that were best estimated using hyperspectral derived vegetation indices were "control" with a RMSEP of 0.4 kg/m<sup>2</sup> ( $R^2 = 0.70$ ,  $RMSEP_{rel} = 7.35$ ), 0.44 kg/m<sup>2</sup> ( $R^2 = 0.87$ ,  $RMSEP_{rel} = 4.88$ ) for ammonium sulfate combined with lime, 0.51 kg/m<sup>2</sup> for ammonium sulfate ( $R^2 = 0.79$ ,  $RMSEP_{rel} = 8.72$ ), and 0.47 kg/m<sup>2</sup>

**Fig. 4.** Accuracy of Sentinel 2 MSI bands and indices in predicting above ground biomass across different fertilizer treatments in relation to accuracies of hyperspectral, Landsat 8 and indices. (a and b) represent the R-square obtained from the using spectral bands and indices, respectively in estimating grass above ground biomass, (c and d) represent root mean square errors of grass above ground biomass prediction derived from raw bands and indices respectively. ALL = all treatments pooled. AN = ammonium nitrate; AS = ammonium sulfate; L = lime; and PL = phosphorus combined with lime.

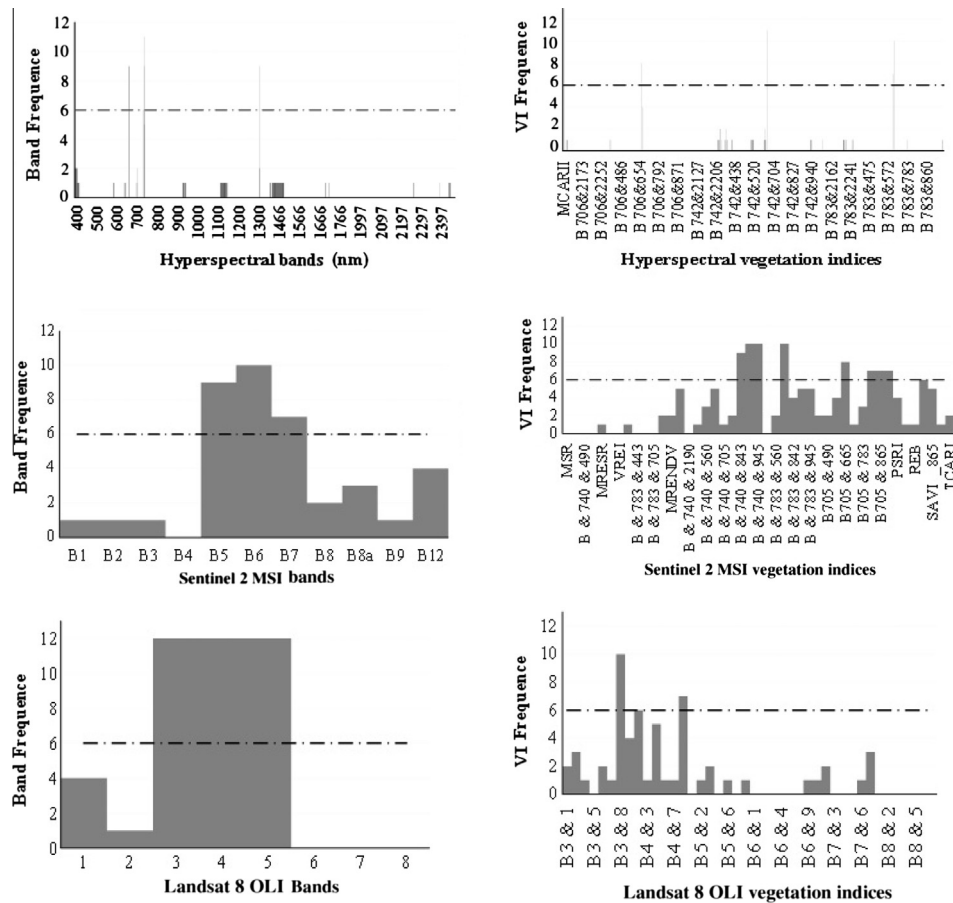


**Fig. 5.** Frequency of raw hyperspectral, Sentinel and Landsat bands in estimating above ground biomass across different fertilizer treatments. The dotted line shows the optimal number of treatments estimated by bands or indices. The optimum number six is the half of the twelve fertilizer treatment combinations.

for Phosphorous ( $R^2 = 0.85$ ,  $RMSEP_{rel} = 8.13$ ). When using Sentinel 2 MSI derived vegetation indices, “control” had a  $RMSEP$  of  $0.89 \text{ kg/m}^2$  ( $R^2 = 0.68$ ,  $RMSEP_{rel} = 16.42$ ),  $0.51 \text{ kg/m}^2$  ( $R^2 = 0.78$ ,  $RMSEP_{rel} = 10.23$ ) for ammonium sulfate combined with phosphorous,  $0.7112 \text{ kg/m}^2$  ( $R^2 = 0.79$ ,  $RMSEP_{rel} = 12.17$ ) for ammonium sulfate and  $0.8963 \text{ kg/m}^2$  ( $R^2 = 0.84$ ,  $RMSEP_{rel} = 15.47$ ) for phosphorous. When using vegetation indices derived from Landsat 8 OLI bands, the ammonium nitrate had a  $RMSEP$  of  $0.66 \text{ kg/m}^2$  ( $R^2 = 0.42$ ,  $RMSEP_{rel} = 17.78$ ),  $0.79 \text{ kg/m}^2$  ( $R^2 = 0.56$ ,  $RMSEP_{rel} = 17.64$ ) for “control”,  $0.84 \text{ kg/m}^2$  ( $R^2 = 0.57$ ,  $RMSEP_{rel} = 17.25$ ) for ammonium sulfate combined with phosphorous (ASP), and  $0.8741 \text{ kg/m}^2$  ( $R^2 = 0.74$ ,  $RMSEP_{rel} = 15.09$ ) for phosphorous. When all the fertilizer treatment were pooled together, vegetation indices derived from the new generation sensors (Sentinel 2 MSI:  $R^2 = 0.76$ ;  $RMSEP = 1.19 \text{ kg/m}^2$ ;  $RMSEP_{rel} = 18.62$  and Landsat 8 OLI:  $R^2 = 0.65$ ;  $RMSEP = 1.17 \text{ kg/m}^2$ ;  $RMSEP_{rel} = 19.41$ ) and hyperspectral data ( $R^2 = 0.92$ ;  $RMSEP = 1.18 \text{ kg/m}^2$ ;  $RMSEP_{rel} = 12.14$ ) optimally estimated grass above ground biomass.

Fig. 5 and Table 5 illustrate the detailed frequency and location of each hyperspectral, Sentinel 2 MSI, and Landsat 8 OLI and vegetation indices within the electromagnetic spectrum that were used in comparing the utility of new generation sensors in estimating above ground biomass of grass treated with different fertilizer combinations. It can be observed that the optimal bands and indices that have a potential to estimate grass above ground biomass across all fertilizer treatments are mainly from the red edge and near infrared sections for all the sensors.

Although this study did not seek to evaluate the utility of new generation sensors in estimating the effect of specific fertilizer

combination treatments on grass above ground biomass, it can be observed that ammonium nitrate as well as the “control” treatments were optimally estimated both when using raw bands and indices derived from the three sensors. In addition, results of this study also showed that red edge and near infrared vegetation indices derived from the three sensors better estimated grass above ground biomass across different fertilizer combinations when compared with raw bands.

### 3.4. Combination of optimal bands and indices derived from Hyperspectral, Sentinel 2 MSI and Landsat 8 OLI

Table 6 shows number of selected bands and indices when using Sentinel 2 MSI, Landsat 8 OLI and hyperspectral data. A total of 9 Sentinel 2 MSI bands and indices were selected. The bulk of the bands and indices that could optimally estimate above ground biomass are close to the chlorophyll absorption regions of the red edge (700–780 nm). In particular, B5, B6, NDVI705 and 665, B8a & 865, B8a SAVI were selected from Sentinel 2 MSI whereas for the hyperspectral data 740, 741, 1310 nm, ndvi742\_665, 706\_437 and 742\_935 nm were selected as the best. For Landsat 8 OLI, the selected bands were B4, B5, ndvi B4\_5, ndviB4\_8, ndviB5\_4, ndviB5\_8. Based on the combination of the best bands and indices derived in this study, it can be noted that Sentinel 2 MSI performed slightly lower ( $R^2 = 0.81$ ,  $RMSEP = 1.07 \text{ kg/m}^2$ ,  $RMSEP_{rel} = 14.97$ ; than hyperspectral data ( $R^2 = 0.92$ ,  $RMSEP = 0.69 \text{ kg/m}^2$ ,  $RMSEP_{rel} = 9.61$ ). Sentinel performed relatively better than Landsat 8 OLI ( $R^2 = 0.76$ ,  $RMSEP = 1.15 \text{ kg/m}^2$ ,  $RMSEP_{rel} = 16.04$ ). Although Landsat 8 OLI has a slightly higher  $RMSEP$  than Sentinel,

**Table 5**  
Frequency of selected bands that optimally estimate above ground biomass of grasses treated with different fertilizer treatments.

| Treatment                | Visible 390–679 |            |           | RE 680–750 |                |           | NIR 700–1300 |                |           | MID_IR 1300–2500 |                |           | Total bands |                |           |
|--------------------------|-----------------|------------|-----------|------------|----------------|-----------|--------------|----------------|-----------|------------------|----------------|-----------|-------------|----------------|-----------|
|                          | ASD             | Sentinel 2 | Landsat 8 | ASD        | Sentinel 2 MSI | Landsat 8 | ASD          | Sentinel 2 MSI | Landsat 8 | ASD              | Sentinel 2 MSI | Landsat 8 | ASD         | Sentinel 2 MSI | Landsat 8 |
| "Control"                | 0               | 0          | 3         | 1          | 1              | 0         | 1            | 3              | 1         | 5                | 0              | 0         | 6           | 3              | 4         |
| Phosphorous              | 0               | 1          | 3         | 3          | 2              | 0         | 3            | 3              | 1         | 2                | 0              | 0         | 5           | 4              | 4         |
| Lime                     | 13              | 0          | 2         | 5          | 1              | 0         | 5            | 3              | 1         | 1                | 1              | 0         | 19          | 3              | 3         |
| PL                       | 2               | 0          | 2         | 2          | 2              | 0         | 2            | 2              | 1         | 8                | 0              | 0         | 12          | 3              | 3         |
| AN                       | 2               | 0          | 2         | 6          | 2              | 0         | 6            | 2              | 1         | 1                | 1              | 0         | 9           | 3              | 3         |
| AS                       | 24              | 0          | 3         | 1          | 2              | 0         | 1            | 3              | 1         | 5                | 0              | 0         | 30          | 3              | 4         |
| ANL                      | 2               | 0          | 2         | 4          | 2              | 0         | 4            | 3              | 1         | 0                | 1              | 0         | 6           | 4              | 3         |
| ASL                      | 2               | 0          | 3         | 5          | 2              | 0         | 5            | 3              | 1         | 1                | 0              | 0         | 8           | 3              | 4         |
| ANP                      | 6               | 0          | 2         | 5          | 0              | 0         | 55           | 3              | 1         | 67               | 1              | 0         | 128         | 4              | 3         |
| ASP                      | 2               | 0          | 3         | 4          | 2              | 0         | 4            | 3              | 1         | 1                | 0              | 0         | 7           | 3              | 4         |
| ANLP                     | 7               | 1          | 2         | 3          | 2              | 0         | 3            | 2              | 1         | 0                | 0              | 0         | 10          | 3              | 3         |
| ASLP                     | 2               | 1          | 2         | 2          | 1              | 0         | 2            | 3              | 1         | 2                | 0              | 0         | 6           | 3              | 3         |
| All treatments           | 0               | 0          | 3         | 2          | 2              | 0         | 2            | 3              | 1         | 1                | 0              | 0         | 3           | 3              | 4         |
| Combined Bands & indices | 0               | 0          | 4(1B&3I)  | 4(2B&4I)   | 5(2B & 2I)     | 0         | 7(2B&5I)     | 5(2B & 4I)     | 3(1B&2I)  | 1                | 0              | 11        | 8           | 9              | 7         |

no significant differences ( $p < 0.05$ ) were observed in terms of accuracy between the two new generation sensors (Fig. 6).

#### 4. Discussion

This study sought to explore the utility of the new generation multispectral sensor, Sentinel 2 MSI in estimating biomass across different fertilizer treatments. We then compared findings with those obtained using Landsat 8 OLI simulated data, and hyperspectral data in order to understand the productivity of native grasslands treated with different fertilizer combinations.

##### 4.1. Combination of optimal bands and indices derived from Hyperspectral, Sentinel 2 MSI and Landsat 8 OLI

The present study has shown that the best Sentinel 2 MSI bands and indices that optimally estimated grass above ground biomass across the twelve fertilizer combinations are from the red edge (bands 4, 5 and 8a), similar to those of hyperspectral (705, 706, 740 and 741). Relatively, the optimal bands that were selected for Landsat 8 OLI (bands 4 and 5) were in the near infrared region. All these selected bands are within wavelength regions that are known to relate well with biomass (Curran, 1989; Mutanga et al., 2005; Ramoelo et al., 2013). As in other earlier related studies (Curran et al., 2001; Mutanga and Skidmore, 2004a, 2007), the high influence of near infrared bands at the canopy level can be explained by the high nitrogen concentration in the ammonium fertilizers (33% in ammonium nitrate and 21% in ammonium sulfate fertilizer), which increased biomass density, leaf area Index (LAI) and leaf area distribution (LAD). For instance, nitrogen stimulates rapid growth and plant healthy (Fichtner and Schulze, 1992; Bassegio et al., 2013) and the red edge/NIR region is sensitive to such changes. Clevers and Gitelson (2013), demonstrated the significance of Sentinel 2 MSI red edge bands centered at 705 and 740 nm in optimally estimating chlorophyll and nitrogen in grasslands and crops. The results of this study are consistent with those of Delegido et al. (2011) who also indicated a strong influence of Sentinel 2 MSI's new red edge bands as well as the derived normalized difference vegetation indices in estimating the leaf area and chlorophyll of crops. In a related study, Ramoelo et al. (2014) also noted that Sentinel 2 MSI red edge bands could optimally estimate leaf nitrogen in the north eastern part of South Africa.

##### 4.2. Evaluating the performance of Sentinel 2 MSI in estimating grass above ground biomass relative to other sensors

Although hyperspectral data outperformed the new generation sensors, its utility is prohibited by the high cost, area coverage, multi-collinearity and dimensionality (Adjorlolo et al., 2015). This study has shown that Sentinel 2 MSI and Landsat 8 OLI, which are freely available and cover large swath widths, can still yield acceptable biomass estimation accuracies. The variations in prediction accuracies among sensors can be explained by the differences in the bandwidths. Specifically, hyperspectral data is measured at 1.4 nm intervals at region 350–1000 nm and at 2 nm intervals within the wavelength region 1000–2500 nm (Abdel-Rahman et al., 2014). Comparatively, the bandwidths of the new generation sensors are marginally different from those of traditional sensors. Sentinel 2 MSI has a bandwidth ranging from 50 to 180 nm for its 12 bands (Delegido et al., 2011), hyperspectral has bandwidths that range from approximately 1 nm. In that regard, it was implicit that hyperspectral sensor derived bands and indices would perform somewhat better than the new generation sensors. However, the findings of this study underscore the potential of new generation sensors, Sentinel 2 MSI and Landsat 8 OLI, in estimating grass



**Table 6**

Selected bands and indices that can be used to optimally estimate grass above ground biomass across different fertilizer combinations and their relation to known biomass related wavelengths.

| Absorption feature center | Wavelength of chemical influence | Known casual biochemical | Reference   | All selected bands   | Frequency of bands/indices selected of known wavelength |
|---------------------------|----------------------------------|--------------------------|---|--|---|
| 550–700                   | Red edge                         | Chlorophyll + nitrogen   | Barnes et al. (2000)  | Sentinel: B5_705, <b>B6_740</b> , NDVI705_665, ndvi705_945, <b>ndvi740_945</b> | 5   |
| 700–750                   | Foliage, biomass                 |                          | Blackburn and Steele (1999)<br>Gitelson and Merzlyak (2003)                   | Landsat 8: B4, <b>B5</b> , ndvi B4_5, ndviB4_8, <b>ndviB5_4</b> , ndviB5_8     | 7   |
| 680/670                   | Carotenoids                      |                          | Sims and Gamon (2002)<br>and Adam et al. (2014)<br>van Deventer et al. (2015) | ASD: <b>B740</b> , <b>B741</b> , ndvi706_437, ndvi742_935, <b>ndvi742_665</b>  | 5   |
| 860                       | Leaf water content               |                          | Blackburn and Steele (1999)<br>van Deventer et al. (2015)                     | Sentinel: <b>B8a_865</b> , SAVI_865  | 4   |
|                           |                                  |                          |   | ASD: ndvi783_665, <b>ndvi783_667</b> , B1310                                   | 3   |
| Total                     |                                  |                          |   |  | 26  |

The similar optimal wavelengths across the three sensors are represented in bold.

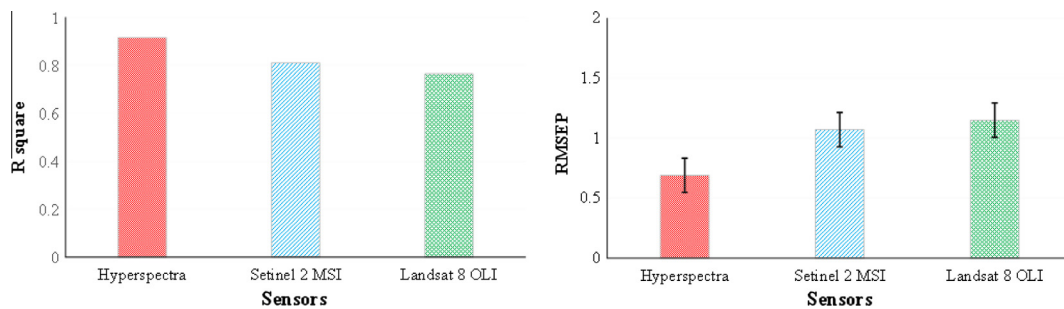


**Fig. 6.** Comparison of new generation and traditional sensors in estimating grass above ground biomass across all (pooled) fertilizer treatments using a combination of the selected best bands and vegetation indices derived from hyperspectral data, Sentinel and Landsat 8. Error plots represent the upper and the lower confidence intervals of each sensor's prediction error.

above ground biomass at a regional scale despite their intermediate spectral resolutions. Results of this study are comparable to the results of Numata et al. (2007) who also estimated grass above ground biomass with plausible accuracies ( $R^2 = 0.72$ ) similar to those presented in this study. Although Landsat 8 OLI data may be used as an alternative to Sentinel 2 MSI, the red edge bands on Sentinel 2 MSI sensor offer great potential for biomass estimation, a component that previously limited the utility of multispectral sensors. Moreover, in resource scarce regions where costs of data over ride the need for optimal spectral resolutions in remote sensing above ground biomass (Lu, 2006; Dube and Mutanga, 2015a; Dube et al., 2017), the high costs of hyperspectral sensors hails high the potential of Sentinel 2 MSI in rangeland ecology. Proper rangeland management techniques require cheap, timely and accurate data that is repeatedly collected at regional scales (Mansour et al., 2012). Considering the expenses associated with hyperspectral sensors as well as their limitation to a local scale, hyperspectral sensors are, to some extent, inappropriate for rangeland management activities in sub Saharan Africa (Mansour et al., 2012). In view of this study's findings, there is still a need to compare and understand the utility of these sensors, paying particular interest to the variations in terms of spatial fidelity in estimating grass above ground biomass at a regional scale.

Results of this study also point out that ammonium nitrate and "control" treatments were the best treatments that could be optimally predicted constantly across the three sensors, both using the raw bands as well as the derived vegetation indices. As mentioned above, the nitrogen/phosphorous/potassium ratio of ammonium

fertilizer is 33-0-0. Considering the fact that nitrogen has been proven to be one of the fertilizers that results in rapid plant growth rate, LAI, LAD and more importantly high accumulation of biomass density, the relatively high nitrogen content could therefore explain optimal estimation of biomass using the three sensors.

Finally, the results of this study indicated that vegetation indices out performed raw spectral bands in estimating grass above ground biomass across all fertilizer treatments. A large body of literature has demonstrated the utility and robustness of vegetation indices in estimating above ground biomass (Mutanga and Skidmore, 2004b; Clevers and Gitelson, 2013; Helman et al., 2014; Ren and Feng, 2014). The plausible performance of vegetation indices could be attributed to their ability to reduce background effects much better than individual spectral bands. In addition, vegetation indices are more sensitive to plant biochemical and biophysical differences. This could be explained by that vegetation indices are a product of two or more bands that are more sensitive to vegetation traits as compared with single bands that may be tainted by background effects hence poorly estimate biomass (Bannari et al., 1995). For instance, normalized vegetation index used in this study is a result of the red and red edge bands as well as near infrared bands. The visible red radiation is absorbed by plants' chlorophyll while the near infrared radiation is highly reflected by vegetation leaves. Thus a combination of these two portions of the wavelengths results in a much robust index that can optimally estimate plant biomass than singular bands that are susceptible to back ground effects hence their unsatisfactory performance in this study.

## 5. Conclusion

This study sought to explore the utility of the forth coming new generation multispectral sensor Sentinel 2 MSI performance in estimating grass above ground biomass across different fertilizer treatments in relation to the performance of new Landsat 8 OLI and hyperspectral. Grounded on the results of this study, we conclude that the red edge bands 4, 5 and 8a of Sentinel 2 MSI could be effectively used to optimally and consistently estimate biomass across all fertilizer combinations compared to hyperspectral data (bands 705, 706, 740 and 741 nm).

This study demonstrates the potential of new generation multispectral sensors in effectively estimating above ground biomass for optimal rangeland management purposes. The findings of this study are a footing for regional grass quantity evaluation which is essential in the livestock industry. Despite the fact that the findings of this study need to be tested at a regional scale to compare the spatial fidelity of these sensors, this work provides a basis for efficient evaluation of grass quantity at a regional scale. The red edge and near infrared wavelengths established in this work underscore the potential of the new multispectral sensor bands in rangeland resource monitoring and management.

## Acknowledgements

The authors are grateful to the KwaZulu-Natal Sandstone Sourveld (KZNSS) and eThekweni Municipality in conjunction with the Inyvesi Yakwazulu-Natali for funding this research. Authors would also like to thank Prof. Dr. K. Kirkman, Craig Morris, Alison Young, Dr. R. Ismail, Dr. Elhadi Adam, Dr. Abdel-Rahman E.M., Dr. T. Dube, Dr. Khoboso, E. Seutloali, Victor M. Bangamwabo, Kusasa Sithole, Nokuphila L.S. Buthelezi, Reneilwe Maake, Ndoni Mgunu and Perushen Rajah for assistance with field work, data collection and analysis. Finally, the authors extend their gratitude to the anonymous reviewers for their constructive criticism.

## References

- Abbasi, A.Z. et al., 2014. A review of wireless sensors and networks' applications in agriculture. *Comput. Stand. Interface* 36 (2), 263–270.
- Abdel-Rahman, E.M. et al., 2014. A comparison of partial least squares (PLS) and sparse PLS regressions for predicting yield of Swiss chard grown under different irrigation water sources using hyperspectral data. *Comput. Electr. Agric.* 106, 11–19.
- Adam, E. et al., 2014. Estimating standing biomass in papyrus (*Cyperus papyrus* L.) swamp: exploratory of in situ hyperspectral indices and random forest regression. *Int. J. Remote Sens.* 35 (2), 693–714.
- Adjorlolo, C. et al., 2015. Predicting C3 and C4 grass nutrient variability using in situ canopy reflectance and partial least squares regression. *Int. J. Remote Sens.* 36 (6), 1743–1761.
- Agapiou, A. et al., 2012. Evaluation of broadband and narrowband vegetation indices for the identification of archaeological crop marks. *Remote Sens.* 4 (12), 3892–3919.
- Anderson, G.L. et al., 1993. Evaluating landsat thematic mapper derived vegetation indices for estimating above-ground biomass on semiarid rangelands. *Remote Sens. Environ.* 45 (2), 165–175.
- Bannari, A. et al., 1995. A review of vegetation indices. *Remote Sens. Rev.* 13 (1–2), 95–120.
- Barnes, E. et al., 2000. Coincident detection of crop water stress, nitrogen status and canopy density using ground based multispectral data. In: *Proceedings of the Fifth International Conference on Precision Agriculture*, Bloomington, IN, USA.
- Bassegio, D. et al., 2013. Effect of nitrogen fertilization and cutting age on yield of tropical forage plants. *Afr. J. Agric. Res.* 8, 1427–1432.
- Blackburn, G.A., Steele, C.M., 1999. Towards the remote sensing of matorral vegetation physiology: relationships between spectral reflectance, pigment, and biophysical characteristics of semiarid bushland canopies. *Remote Sens. Environ.* 70 (3), 278–292.
- Broge, N.H., Leblanc, E., 2001. Comparing prediction power and stability of broadband and hyperspectral vegetation indices for estimation of green leaf area index and canopy chlorophyll density. *Remote Sens. Environ.* 76 (2), 156–172.
- Broge, N.H., Mortensen, J.V., 2002. Deriving green crop area index and canopy chlorophyll density of winter wheat from spectral reflectance data. *Remote Sens. Environ.* 81 (1), 45–57.
- Cho, M., et al., 2008. Discriminating species using hyperspectral indices at leaf and canopy scales. In: *Proc. ISPRS Congr.*, Beijing, pp. 369–376.
- Chun, H., Keleş, S., 2010. Sparse partial least squares regression for simultaneous dimension reduction and variable selection. *J. R. Stat. Soc. Series B Stat. Methodol.* 72 (1), 3–25.
- Clevers, J.G., Gitelson, A.A., 2013. Remote estimation of crop and grass chlorophyll and nitrogen content using red-edge bands on Sentinel-2 and -3. *Int. J. Appl. Earth Obs. Geoinf.* 23, 344–351.
- Cole, B., et al., 2014. Delivering the Copernicus land monitoring service, production of the CORINE Land Cover Map in the UK. A Forward Looking Perspective to the Sentinel-2 Mission. *EGU General Assembly Conference Abstracts*.
- Curran, P.J., 1989. Remote sensing of foliar chemistry. *Remote Sens. Environ.* 30 (3), 271–278.
- Curran, P.J., 2001. Imaging spectrometry for ecological applications. *Int. J. Appl. Earth Obs. Geoinf.* 3 (4), 305–312.
- Curran, P.J. et al., 2001. Estimating the foliar biochemical concentration of leaves with reflectance spectrometry: testing the Kokaly and Clark methodologies. *Remote Sens. Environ.* 76 (3), 349–359.
- Delegido, J. et al., 2011. Evaluation of Sentinel-2 red-edge bands for empirical estimation of green LAI and chlorophyll content. *Sensors* 11 (7), 7063–7081.
- Dube, T., Mutanga, O., 2015a. Evaluating the utility of the medium-spatial resolution Landsat 8 multispectral sensor in quantifying aboveground biomass in uMgeni catchment, South Africa. *ISPRS J. Photogramm. Remote Sens.* 101, 36–46.
- Dube, T., Mutanga, O., 2015b. Investigating the robustness of the new Landsat-8 operational land imager derived texture metrics in estimating plantation forest aboveground biomass in resource constrained areas. *ISPRS J. Photogramm. Remote Sens.* 108, 12–32.
- Dube, T., Mutanga, O., Ismail, R., 2017. Quantifying aboveground biomass in African environments: a review of the trade-offs between sensor estimation accuracy and costs. *Trop. Ecol.* 57 (2).
- Elvidge, C.D., Chen, Z., 1995. Comparison of broad-band and narrow-band red and near-infrared vegetation indices. *Remote Sens. Environ.* 54 (1), 38–48.
- Fichtner, K., Schulze, E.D., 1992. The effect of nitrogen nutrition on growth and biomass partitioning of annual plants originating from habitats of different nitrogen availability. *Oecologia* 92 (2), 236–241.
- Fynn, R.W., O'Connor, T.G., 2005. Determinants of community organization of a South African mesic grassland. *J. Veg. Sci.* 16 (1), 93–102.
- Ghani, A. et al., 2014. Agronomic assessment of gibberellic acid and cytokinin plant growth regulators with nitrogen fertiliser application for increasing dry matter production and reducing the environmental footprint. In: *Proceedings of the New Zealand Grassland Association*.
- Gitelson, A.A., Merzlyak, M.N., 2003. Relationships between leaf chlorophyll content and spectral reflectance and algorithms for non-destructive chlorophyll assessment in higher plant leaves. *J. Plant Physiol.* 160 (3), 271–282.
- Haboudane, D. et al., 2002. Integrated narrow-band vegetation indices for prediction of crop chlorophyll content for application to precision agriculture. *Remote Sens. Environ.* 81 (2–3), 416–426.
- Hansen, P.M., Schjoerring, J.K., 2003. Reflectance measurement of canopy biomass and nitrogen status in wheat crops using normalized difference vegetation indices and partial least squares regression. *Remote Sens. Environ.* 86 (4), 542–553.
- Helman, D. et al., 2014. Detecting changes in biomass productivity in a different land management regimes in drylands using satellite-derived vegetation index. *Soil Use Manag.* 30 (1), 32–39.
- Jørgensen, M., et al., 2014. Effect of climatic changes on grassland growth, water condition and biomass—the FINEGRASS project. EGF at 50: The future of European grasslands. In: *Proceedings of the 25th General Meeting of the European Grassland Federation*, Aberystwyth, Wales, 7–11 September 2014, IBERS, Aberystwyth University.
- Kooistra, L. et al., 2010. Assessment of the biomass and nitrogen status of natural grasslands using hyperspectral remote sensing.
- Lachérade, S., et al., 2014. Introduction to the Sentinel-2 radiometric calibration activities during commissioning phase.
- Laurent, V.C.E. et al., 2014. Bayesian object-based estimation of LAI and chlorophyll from a simulated Sentinel-2 top-of-atmosphere radiance image. *Remote Sens. Environ.* 140, 318–329.
- Lee, D. et al., 2011. Sparse partial least-squares regression and its applications to high-throughput data analysis. *Chemom. Intell. Lab. Syst.* 109 (1), 1–8.
- Li, X. et al., 2014. Super-resolution mapping of forests with bitemporal different spatial resolution images based on the spatial-temporal Markov random field. *IEEE J. Sel. Top. Appl. Earth Obs. Remote Sens.* 7 (1), 29–39.
- Ling, B. et al., 2014. Estimating canopy nitrogen content in a heterogeneous grassland with varying fire and grazing treatments: Konza Prairie, Kansas, USA. *Remote Sens.* 6 (5), 4430–4453.
- Liu, Z.Y. et al., 2007. Comparison of vegetation indices and red-edge parameters for estimating grassland cover from canopy reflectance data. *J. Integr. Plant Biol.* 49 (3), 299–306.
- Lu, D., 2005. Aboveground biomass estimation using Landsat TM data in the Brazilian Amazon. *Int. J. Remote Sens.* 26 (12), 2509–2525.
- Lu, D., 2006. The potential and challenge of remote sensing-based biomass estimation. *Int. J. Remote Sens.* 27 (7), 1297–1328.
- Mansour, K. et al., 2012. Remote sensing based indicators of vegetation species for assessing rangeland degradation: opportunities and challenges. *Afr. J. Agric. Res.* 7, 3261–3270.

- Moran, M.S. et al., 1997. Opportunities and limitations for image-based remote sensing in precision crop management. *Remote Sens. Environ.* 61 (3), 319–346.
- Morris, C., Fynn, R., 2001. The Ukulinga long-term grassland trials: reaping the fruits of meticulous, patient research. *Bull. Grassl. Soc. South. Africa* 11 (1), 7–22.
- Mutanga, O., Adam, E., 2011. High density biomass estimation: testing the utility of Vegetation Indices and the Random Forest Regression algorithm. In: 34th International Symposium for Remote Sensing of the Environment (ISRSE), Sydney, Australia.
- Mutanga, O. et al., 2015. Evaluating the robustness of models developed from field spectral data in predicting African grass foliar nitrogen concentration using WorldView-2 image as an independent test dataset. *Int. J. Appl. Earth Obs. Geoinf.* 34, 178–187.
- Mutanga, O. et al., 2005. Estimating tropical pasture quality at canopy level using band depth analysis with continuum removal in the visible domain. *Int. J. Remote Sens.* 26 (6), 1093–1108.
- Mutanga, O., Skidmore, A.K., 2004a. Hyperspectral band depth analysis for a better estimation of grass biomass (*Cenchrus ciliaris*) measured under controlled laboratory conditions. *Int. J. Appl. Earth Obs. Geoinf.* 5 (2), 87–96.
- Mutanga, O., Skidmore, A.K., 2004b. Narrow band vegetation indices overcome the saturation problem in biomass estimation. *Int. J. Remote Sens.* 25 (19), 3999–4014.
- Mutanga, O., Skidmore, A.K., 2007. Red edge shift and biochemical content in grass canopies. *ISPRS J. Photogramm. Remote Sens.* 62 (1), 34–42.
- Numata, I. et al., 2007. Characterization of pasture biophysical properties and the impact of grazing intensity using remotely sensed data. *Remote Sens. Environ.* 109 (3), 314–327.
- Oumar, Z., Mutanga, O., 2013. Using WorldView-2 bands and indices to predict bronze bug (*Thaumastocoris peregrinus*) damage in plantation forests. *Int. J. Remote Sens.* 34 (6), 2236–2249.
- Porter, T.F. et al., 2014. Estimating biomass on CRP pastureland: a comparison of remote sensing techniques. *Biomass Bioenergy* 66, 268–274.
- Prado, A.D., et al., 2014. Synergies between mitigation and adaptation to climate change in grassland-based farming systems. EGF at 50: The future of European grasslands. In: Proceedings of the 25th General Meeting of the European Grassland Federation, Aberystwyth, Wales, 7–11 September 2014, IBERS, Aberystwyth University.
- Quan, Q. et al., 2015. Nitrogen enrichment and grazing accelerate vegetation restoration in degraded grassland patches. *Ecol. Eng.* 75, 172–177.
- Ramoelo, A. et al., 2014. A Potential for the Spectral Configurations of Sentinel-2 to Assess Rangeland Quality. *International Society for Optics and Photonics, SPIE Remote Sensing*.
- Ramoelo, A. et al., 2013. Non-linear partial least square regression increases the estimation accuracy of grass nitrogen and phosphorus using in-situ hyperspectral and environmental data. *ISPRS J. Photogramm. Remote Sens.* 82, 27–40.
- Ramoelo, A. et al., 2012. Regional estimation of savanna grass nitrogen using the red-edge band of the spaceborne RapidEye sensor. *Int. J. Appl. Earth Obs. Geoinf.* 19, 151–162.
- Ren, H., Feng, G., 2014. Are soil-adjusted vegetation indices better than soil-unadjusted vegetation indices for above-ground green biomass estimation in arid and semi-arid grasslands? *Grass Forage Sci.* 70 (4), 611–619.
- Richardson, A.J. et al., 1983. Radiometric estimation of biomass and nitrogen content of Alicia grass. *Remote Sens. Environ.* 13 (2), 179–184.
- Serrano, L. et al., 2002. Remote sensing of nitrogen and lignin in Mediterranean vegetation from AVIRIS data: decomposing biochemical from structural signals. *Remote Sens. Environ.* 81 (2–3), 355–364.
- Sims, D.A., Gamon, J.A., 2002. Relationships between leaf pigment content and spectral reflectance across a wide range of species, leaf structures and developmental stages. *Remote Sens. Environ.* 81 (2), 337–354.
- Thenkabail, P.S. et al., 2013. Selection of hyperspectral narrowbands (HNBS) and composition of hyperspectral twoband vegetation indices (HVLs) for biophysical characterization and discrimination of crop types using field reflectance and Hyperion/EO-1 data. *IEEE J. Sel. Top. Appl. Earth Obs. Remote Sens.* 6 (2), 427–439.
- Tong, Q. et al., 2014. Progress in hyperspectral remote sensing science and technology in China over the past three decades. *IEEE J. Sel. Top. Appl. Earth Obs. Remote Sens.* 7 (1), 70–91.
- Trotter, M. et al., 2014. Spatial variability in pH and key soil nutrients: is this an opportunity to increase fertiliser and lime-use efficiency in grazing systems? *Crop Pasture Sci.* 65 (8), 817–827.
- Ullah, S. et al., 2012. Estimation of grassland biomass and nitrogen using MERIS data. *Int. J. Appl. Earth Obs. Geoinf.* 19, 196–204.
- Underwood, E.C. et al., 2007. A comparison of spatial and spectral image resolution for mapping invasive plants in coastal California. *Environ. Manage.* 39 (1), 63–83.
- Valentin, K.M. et al., 2014. Response to fertilizer of native grasses (*Pennisetum polystachion* and *Setaria sphacelata*) and legume (*Tephrosia pedicellata*) of savannah in Sudanian Benin. *Fisheries* 3 (3), 142–146.
- van der Meer, F.D. et al., 2014. Potential of ESA's Sentinel-2 for geological applications. *Remote Sens. Environ.* 148, 124–133.
- van Deventer, H. et al., 2015. Capability of models to predict leaf N and P across four seasons for six sub-tropical forest evergreen trees. *ISPRS J. Photogramm. Remote Sens.* 101, 209–220.
- Vickery, P.J. et al., 1980. Assessment of the fertilizer requirement of improved pasture from remote sensing information. *Remote Sens. Environ.* 9 (2), 131–148.
- Vogeler, I. et al., 2014. Effects of fertiliser nitrogen management on nitrate leaching risk from grazed dairy pasture. In: Proceedings of the New Zealand Grassland Association.
- Wight, J.R., Godfrey, E.B., 1985. Predicting yield response to nitrogen fertilization on northern Great Plains rangelands. *J. Range Manage.*, 238–241.
- Yahdjian, L. et al., 2014. Grasses have larger response than shrubs to increased nitrogen availability: a fertilization experiment in the Patagonian steppe. *J. Arid Environ.* 102, 17–20.